



**HAL**  
open science

## Three distinct sub-nuclear populations of HMG-I protein of different properties revealed by co-localization image analysis.

C Amirand, A Viari, J Ballini, Human Rezaei, Nathalie Beaujean, D. Jullien, E. Kas, P. Debey

### ► To cite this version:

C Amirand, A Viari, J Ballini, Human Rezaei, Nathalie Beaujean, et al.. Three distinct sub-nuclear populations of HMG-I protein of different properties revealed by co-localization image analysis.. *Journal of Cell Science*, 1998, 111 ( Pt 23), pp.3551-3561. hal-02610659

**HAL Id: hal-02610659**

**<https://hal.science/hal-02610659>**

Submitted on 17 May 2020

**HAL** is a multi-disciplinary open access archive for the deposit and dissemination of scientific research documents, whether they are published or not. The documents may come from teaching and research institutions in France or abroad, or from public or private research centers.

L'archive ouverte pluridisciplinaire **HAL**, est destinée au dépôt et à la diffusion de documents scientifiques de niveau recherche, publiés ou non, émanant des établissements d'enseignement et de recherche français ou étrangers, des laboratoires publics ou privés.

## Three distinct sub-nuclear populations of HMG-I protein of different properties revealed by co-localization image analysis

Claudine Amirand<sup>1</sup>, Alain Viari<sup>2</sup>, Jean-Pierre Ballini<sup>1,\*</sup>, Human Rezaei<sup>3</sup>, Nathalie Beaujean<sup>3</sup>, Denis Jullien<sup>4,†</sup>, Emmanuel Käs<sup>4</sup> and Pascale Debey<sup>3,§</sup>

<sup>1</sup>Laboratoire de Physicochimie Biomoléculaire et Cellulaire, ESA 7033 CNRS, Université Pierre et Marie Curie, 75005 Paris, France

<sup>2</sup>Atelier de Bioinformatique, Université Pierre et Marie Curie, 75005 Paris, France

<sup>3</sup>Unité INRA 806, Muséum National d'Histoire Naturelle, Institut de Biologie Physico-Chimique, 13 rue Pierre et Marie Curie, 75005 Paris, France

<sup>4</sup>Laboratoire de Biologie Moléculaire Eucaryote, UPR 9006 CNRS, 118 route de Narbonne, 31062 Toulouse Cedex, France

\*Present address: Visiting Professor, Swiss Federal Institute of Technology, EPLF-DRG-LPAS, Lausanne, Switzerland

†Present address: Institute of Cell & Molecular Biology, University of Edinburgh, Swann Building, The King's Buildings, Mayfield Road, Edinburgh EH9 3JR, Scotland, UK

§Author for correspondence

Accepted 2 October; published on WWW 12 November 1998

### SUMMARY

We have studied the nuclear distribution of the non-histone HMG-I protein by indirect immunofluorescence in several human and murine somatic cell lines and in growing mouse oocytes. We show that HMG-I, a high mobility-group protein which interacts *in vitro* with the minor groove of AT-rich B-DNA, is found exclusively in the nucleus and that this localization corresponds to a complex distribution. By comparing the HMG-I-dependent fluorescence signal with the chromatin density determined by Hoechst 33342 or propidium iodide staining, we present evidence for the existence of three HMG-I sub-populations whose contribution to the total fluorescence can be determined using a newly developed quantitative co-localization image analysis program: foci that correspond to regions of

heterochromatin, intense dots located within decondensed chromatin, and a more diffuse component extending throughout the nucleoplasm. In addition, we show that these sub-populations differ in their sensitivity to nuclease digestion and *in vivo* displacement by the minor-groove binder Hoechst 33342. Finally, double immunolabeling of RNA polymerase II-dependent transcription and HMG-I shows that the intense dots are not correlated with sites of high transcriptional activity. We discuss the possibility that these three sub-populations reflect distinct and separable biological functions of the HMG-I protein.

Key words: HMG-I, Co-localization software, Image analysis, Nuclear compartment

### INTRODUCTION

The high mobility-group (HMG) proteins are a group of small, highly charged non-histone chromosomal proteins, which can be sub-divided in three families: HMG-1/-2, HMG-14/-17 and HMG-I(Y) (for review see Bustin and Reeves, 1996). Although their structure and DNA binding properties have been characterized quite well, their function is less understood. It is generally admitted that they act as 'architectural' components that influence different levels of chromatin structure (Bustin and Reeves, 1996). The mammalian HMG-I(Y) family comprises three members: HMG-I (107 amino acids, 11.9 kDa), HMG-Y (96 amino acids, 10.6 kDa), derived from HMG-I by an internal deletion of 11 amino acids, and HMG-IC coded by another gene. All three proteins bind AT-rich DNA through specific binding domains, termed 'AT hooks' (Reeves and Nissen, 1990). *In vitro* studies have shown that HMG-I interacts with the minor groove of AT-rich sequences in B-DNA requiring 5 to 6 consecutive dA.dT base pairs (Reeves and Nissen, 1990; Radic et al., 1992; Strauss and Varshavsky,

1984). Such sequences are particularly abundant in certain satellite DNA repeats and in scaffold-associated regions (SARs) (Zhao et al., 1993). In fact, HMG-I was first isolated on the basis of its interaction with AT-rich regions of green monkey satellite DNA (Strauss and Varshavsky, 1984) and was suggested to play a role in the phasing of nucleosomes. It was also shown to bind quite avidly to SARs *in vitro*, where it antagonizes efficiently histone H1 binding and further assembly into flanking sequences (Zhao et al., 1993; Käs et al., 1989; Izaurrealde et al., 1989). HMG-I could then be an efficient competitor of H1-mediated general repression of transcription (Käs et al., 1993; Zhao et al., 1993). However, these experiments were performed *in vitro* in a non-nucleosomal DNA context and the *in vivo* biological relevance of these findings remains to be established.

HMG-I has also been shown to interact directly with the promoter regions of a limited number of genes such as interferon- $\beta$  (IFN- $\beta$ ) (Thanos and Maniatis, 1992), the  $\alpha$ -chain of the interleukin-2 (IL-2) receptor (John et al., 1995), interleukine-4 (IL-4) (Klein-Hessling et al., 1996), E-selectin

(Ghersa et al., 1997). In addition HMG-I is involved in the activation of the latency-active promoter 2 of Herpes Simplex virus by facilitating the binding of Sp1 (French et al., 1996). In these cases, HMG-I seems to act as an architectural factor required for the proper binding of specific transcription factors through binding-induced modifications of DNA bending (Falvo et al., 1995; Thanos and Maniatis, 1995), and/or through direct protein/protein interactions (John et al., 1995; Leger et al., 1995).

These observations suggest that the specific interaction of HMG-I with AT-rich DNA might support distinct functions depending on the chromatin contexts in which the protein can be found. While HMG-I has been shown to localize to G/Q- and C-bands of human and mouse mitotic chromosomes (Disney et al., 1989; Saitoh and Laemmli, 1994), only a few studies have dealt with the localization of the protein in interphase nuclei (Disney et al., 1989; Thompson et al., 1995). We therefore undertook a study of the nuclear distribution of endogenous HMG-I protein in mouse somatic or germinal cells and in human somatic cells, with the aim of distinguishing between different sub-nuclear populations that might be related to the different proposed functions of HMG-I. Using a newly developed image analysis program, we show that HMG-I accumulates in three different sub-nuclear domains characterized by different reactivities to nucleases and competition by Hoechst 33342. We analyze the possible correlation between these sub-populations and sites of active transcription.

## MATERIALS AND METHODS

### Cell culture and treatments

Human HeLa cells, human fibroblasts (1BR) and mouse fibroblasts (3T3) were cultured in Dulbecco's MEM supplemented with L-glutamine and 10% fetal calf serum (HeLa and 1BR) or new-born calf serum (3T3). For immunofluorescence detection of HMG-I, cells were grown on coverslips to sub-confluence for about 24 hours. Mouse oocytes from sixteen-day-old mice (genotype C57/CBA) were collected as described (Debey et al., 1993) and kept at 37°C in M2 medium before being fixed and processed.

Transcription sites were detected by incorporation of modified RNA precursors (Wansink et al., 1993). Cells grown to sub-confluence on Cellocate plates were micro-injected in the cytoplasm with BrUTP (100 mM diluted in 2 mM Pipes, pH 7.4, 140 mM KCl) using a Zeiss AIS (automated injection system) equipped with a Sutter P87 capillary puller. Approximately 80 cells were microinjected within 15-30 minutes. In the case of oocytes, BrUTP (same concentration as above) was micro-injected using an Eppendorf micro-injector and Narishige micromanipulators, as already described (Bouniol et al., 1995). Cells and oocytes were then incubated in their respective specific culture medium from 10 to 30 minutes, before being fixed and processed as described below.

### HMG-I protein and antibodies

Recombinant human HMG-I protein was produced in *Escherichia coli* and purified by HPLC (Elton and Reeves, 1986). A polyclonal antibody against HMG-I was obtained from rabbits immunized with purified HMG-I (Eurogentec, Belgium). High-titer serum fractions were affinity-purified against HMG-I protein bound to activated CNBr-Sepharose (Pharmacia). Eluted fractions were tested by western blotting of nuclear extracts prepared from HeLa cells.

### Immunofluorescence labeling

Different protocols of fixation-permeabilization were used for somatic

cells: (1) fixation by paraformaldehyde (PFA; 4%, 15 minutes, room temperature) in phosphate buffer (PBS) and permeabilization either by Triton X-100 (0.1%, 15 minutes, room temperature), or NP40 (0.1%, 10 minutes, 4°C); (2) fixation-permeabilization in ethanol/acetone (1/1, v/v) for 5 minutes at 4°C. Human hepatic cells (HEp-2) purchased from Sanofi Diagnostics Pasteur were already fixed with acetone at 4°C. Oocytes were fixed with 2% PFA for 20 minutes and permeabilized with 0.2% Triton X-100 for 15 minutes at room temperature.

The immunolabeling protocol was the same for somatic cells and oocytes, except that oocytes were manipulated using mouth micropipettes, as already described (Debey et al., 1993). Fixed and permeabilized cells were first blocked for at least 1 hour in PBS containing 2% bovine serum albumin (BSA), before being incubated at 4°C overnight with the purified rabbit anti-HMG-I serum (see above) used at a 1/100 dilution, and 1 hour at room temperature with the secondary antibody (an anti-rabbit IgG(H+L) antibody conjugated to fluorescein (FITC) or lissamine-rhodamine (LRSC), Jackson Immuno Research, used at a 1/100 dilution). They were then counterstained for 30 minutes in 2 µg/ml Hoechst 33342 (HO) or 2 µg/ml propidium iodide (PI). In the latter case, a further digestion by 1 mg/ml RNase at 37°C for 30 minutes was performed. Each step was followed by thorough rinses in PBS. Cells were then postfixed in 2% PFA in PBS for 15 minutes and, after washing, coverslips were mounted in Citifluor.

In depletion experiments, 50 to 200 µg of the purified protein were mixed with 1 µl of the purified antibody, diluted to 100 µl in PBS supplemented with 2% BSA and incubated for 7 hours at 4°C before being centrifuged for 30 minutes in an airfuge. The resulting supernatant was then used as above for immunofluorescence studies.

Immunodetection of BrU incorporated into nascent RNAs was performed as already described (Wansink et al., 1993; Bouniol et al., 1995) by incubating cells overnight at 4°C with a mouse monoclonal anti-BrdU antibody, which also recognizes BrU (Caltag Laboratories, 1/500 dilution). The secondary antibody was a fluorescein-conjugated anti-mouse IgG(H+L) (Jackson Immuno Research), used at a 1/200 dilution for 1 hour. In the case of double-labeling experiments (HMG-I and transcription), incubations were performed simultaneously with both primary antibodies, followed by the secondary antibodies.

### DNase I and micrococcal nuclease treatments

RNase-free-DNase I and micrococcal nuclease (MNase) were purchased from Sigma. Concentrated solutions of RNase-free-DNase I (1 mg/ml or 520 units/ml) and MNase (100 units/ml) were prepared in a 0.125 N HCl solution containing 50% glycerol and in PBS, respectively. After fixation-permeabilization in ethanol/acetone, cells were rinsed for 10 minutes in PBS containing 0.5 mM phenylmethylsulfonyl fluoride (PMSF) before being treated for 15 or 30 minutes at 37°C with different concentrations of RNase-free DNase I or MNase in PBS containing 0.5 mM PMSF and 5 mM MgCl<sub>2</sub> or 1 mM CaCl<sub>2</sub>, respectively. After rinsing twice with PBS, nucleases were inactivated by incubating cells for 10 minutes at 4°C in a solution of 20 mM EDTA.

### Preincubation of live cells and oocytes with Hoechst 33342

3T3 or HeLa cells, grown on coverslips during 24 hours, were incubated for 1 hour in the presence of Hoechst 33342 (HO; 1, 5 or 10 µg/ml) in culture medium without serum, then rinsed, fixed with ethanol/acetone and immunolabeled for HMG-I as above. Mouse oocytes were incubated with 5, 10 and 20 µg/ml HO for 1 hour at 37°C in M2 medium. To control for variations among individuals, oocytes from one mouse were separated into two sets, one control (without HO) and the other incubated with HO. Two experiments were performed for each HO concentration. Oocytes were then rinsed, fixed and processed for immunolabeling as above.

## Fluorescence microscopy

Observations were performed on a Zeiss inverted microscope (Axiovert 35) equipped with Zeiss fluorescence filter sets or with a filter wheel. We used a Zeiss Plan Neofluar  $\times 100$  oil immersion objective (NA=1.30) to visualize the distribution of HMG-I or a Zeiss  $\times 20$  objective (NA=0.5) for quantification of the total fluorescence intensity, respectively. Image acquisition and processing were performed either with an intensified video camera (type 4336, Lhesa Electronique) coupled to a digital Sapphire system (Quantel Consultants) as previously described (Debey et al., 1993), or with a CCD camera (Photometrics type KAF 1400, 12-bit dynamic range), cooled to 10°C and coupled to the IPLAB Spectrum Imaging software. In the latter case, one pixel of an image (658 $\times$ 517 pixels) recorded with a  $\times 100$  objective corresponds to a 0.133  $\mu\text{m} \times$  0.133  $\mu\text{m}$  square. Using a filter wheel for the excitation light and a triple-band dichroic mirror and filter set for emitted light, images from double fluorescent beads taken at two different wavelengths differed at most by a translation of 1 pixel.

Images were acquired after stabilization of the excitation mercury lamp. They were corrected for heterogeneities in the illumination and camera sensitivity by a shading correction, using black and white images captured with the same objective. Confocal imaging microscopy was performed on a Zeiss LSM-310 confocal laser scanning microscope with a Zeiss Plan Neofluar  $\times 63$  oil immersion objective (NA=1.4), using excitation wavelengths of 488 and 543 nm.

## Image analysis

For quantitative measurements of the integrated fluorescence (HMG-I immunolabeling or HO) emitted by each nucleus, images were recorded with the  $\times 20$  objective after a 2 hour stabilization of the mercury lamp. For HMG-I images, the mean intensity of the cytoplasmic area (background) was subtracted from the whole image. This was not necessary in the case of HO as the background fluorescence due to free HO was undetectable. A mask defining the outlines of all nuclei from a given field was then defined by thresholding the HO image and applied on the corresponding HMG-I image. The fluorescence intensity emitted by each individual nucleus was measured at the two wavelengths using the IPLAB software. Data were saved in a file for statistical analysis. Precision on the mean intensity value is expressed through the standard error of the mean ( $P=99\%$ ). As fluorescence gives only relative intensity values, intensities were compared only among images taken within a 4 hour interval.

To study the spatial distribution of two labeled macromolecules (for example HMG-I and chromatin or HMG-I and nascent RNAs), images were recorded at the two selected wavelengths with the  $\times 100$  objective and corrected for spatial heterogeneities as described above. Analysis was performed using the Co-localization Image Analysis program from the SPIMAC ('Spectral Imaging on Macintosh') software developed by A. Viari and J. P. Ballini following a method previously proposed by Taneja et al. (1992) and by Demandoix and Davoust (1995). The software provides a 2-D histogram, similar to the one used in flow cytometry, where  $x$  and  $y$  coordinates represent the gray levels of the same pixel in the two images, respectively.  $x$  and  $y$  values are normalized relative to the highest gray level in each image, which is set to a value of 100. Note that, due to this normalization, intensity values on the 2-D histograms from two different cells cannot be compared. In addition, each point of the histogram is assigned a color on a scale representing the number of pixels with the same pair of gray levels. Different sub-populations can then be identified as different regions of the 2-D histogram, depending on the relative intensities of the two fluorescent probes, and can be delineated by thresholding or by drawing a rectangle or a polygon on the 2-D histogram. Pixels belonging to a given sub-population can then be localized interactively on each of the two initial images. The SPIMAC software also calculates the pixel number of any selected

region of the histogram, as well as the integrated and mean intensities of these pixels in each image.

## RESULTS

### HMG-I localizes to distinct nuclear sites that correspond to different levels of chromatin condensation

The rabbit polyclonal serum used in our studies was raised against recombinant human HMG-I and purified by affinity chromatography against the immobilized purified protein. This antibody reacts highly specifically with HMG-I, as shown by western blots of nuclear HeLa cells extracts (Fig. 1A). An unknown 120 kDa protein is also detected by the antibody, but this cross-reactive band disappears upon a 5-fold dilution of the antibody.

We used a suitable dilution of this antibody for immunofluorescence studies in HeLa and 3T3 cells (Fig. 1B-E) as well as in 1BR and HEP-2 tissue-culture cells (data not shown). In all cases, the antibody revealed an exclusively nuclear localization of HMG-I. No labeling was observed in control experiments performed without incubation with the primary antibody, or following incubation with the pre-immune serum (data not shown). We verified in each experiment the absence of light leak-through from one channel to another and that the HMG-I labeling pattern did not depend on the fixation/permeabilization protocol used. Finally, depletion of the serum by preincubation with purified HMG-I led to the almost complete disappearance of nuclear labeling (Fig. 1F and G). While a large increase in contrast reveals a residual nuclear signal in the form of small dots, its intensity is comparable to that of the cytoplasmic background (data not shown). Therefore, the immunofluorescence signal we detect is indeed due to a highly specific reaction with nuclear HMG-I protein.

Visual observations of the immunolocalization of HMG-I with respect to DNA (stained with Hoechst 33342, HO or propidium iodide, PI), reveal that the HMG-I signal can be subdivided into three components. As shown in Fig. 2, they correspond to relatively intense extranucleolar small dots (about 0.3  $\mu\text{m}$  in diameter) scattered in areas of low HO (or PI) fluorescence intensity, larger foci that coincide with chromocenters of high HO (PI) fluorescence and a continuous labeling of the whole nuclear area. These components, which are most easily distinguished in 3T3 cells and somewhat less so in HeLa cells (Fig. 2, compare A,B and C,D), are also observed in 1BR and HEP-2 cells (data now shown).

Using the SPIMAC software described in Materials and Methods, the distribution of HMG-I with respect to HO intensity was analyzed more precisely on HMG-I/HO 2-D histograms where  $x$  and  $y$  coordinates represent normalized HMG-I and HO fluorescence intensity levels, respectively. The 2-D histograms presented in Fig. 3 are derived from the HMG-I and HO images of the 3T3 and HeLa cells shown in Fig. 2. The three nuclear HMG-I sub-populations described above are evidenced as three different regions of the 2-D histograms: the first region is represented by pixels of high HMG-I and low HO fluorescence intensities, concentrated along one (or sometimes two) horizontal line(s) (Fig. 3A, upper rows). On the HMG-I image, the pixels of this region correspond to the

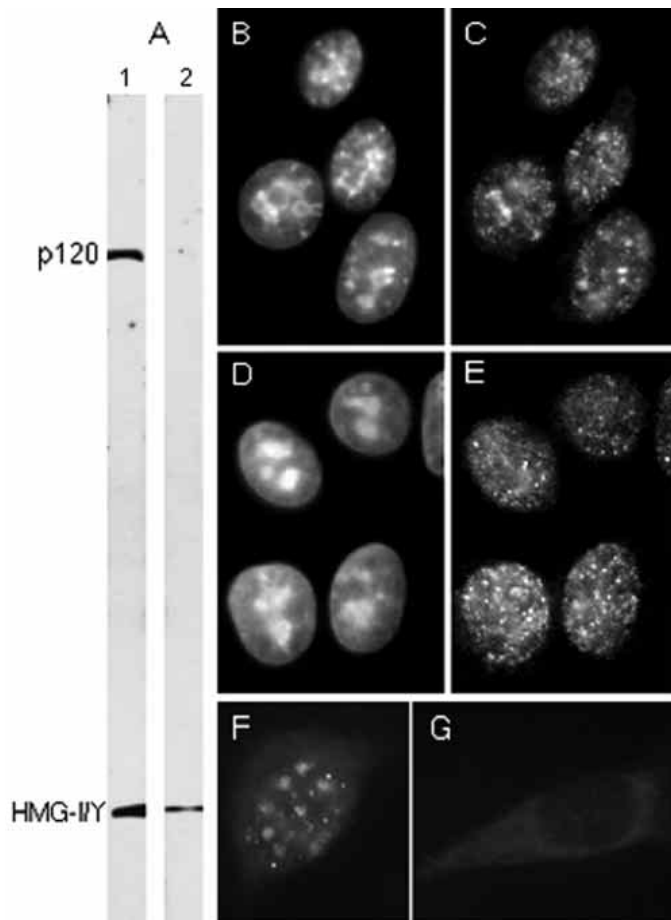


**Fig. 1.** Detection of HMG-I/Y in HeLa cells by western blotting and indirect immunofluorescence. (A) Western blots of nuclear extracts from HeLa cells using pooled fractions of the affinity-purified serum raised against HMG-I. Serum dilutions were 1:100, 1:500 in lanes 1 and 2, respectively. The serum only detects 2 bands: HMG-I and, at the lowest dilution only, an unknown protein of 120 kDa. (B to E) The immunofluorescence pattern of HMG-I in 3T3 cells (C) and in HeLa cells (E), using the same serum and the corresponding staining with Hoechst 33342 (3T3 in B and HeLa in D). HMG-I labeling is concentrated in the nucleus. The HMG-I fluorescence pattern detected in a 3T3 cell after treatment with the serum depleted by preincubation with purified HMG-I is shown in G and can be compared to a control immunofluorescence staining (F) obtained with the same imaging parameters.

small dots described above, which therefore seem to be located in nuclear regions of uniformly low HO intensity. The second region of the 2-D histogram represents pixels of medium HMG-I and intense HO fluorescence (B, middle rows), with a linear correlation between the two signals. When selected, the corresponding pixels of the HMG-I image are those of the foci. Therefore, in contrast to the small dots, the intensity of the HMG-I signal in the foci is proportional to the DNA labeling. The continuous HMG-I staining pattern appears as a third sub-population where HO and HMG-I intensities are again proportional (C, lower rows).

The SPIMAC software also provides quantitative data on the relative area and fluorescence intensity corresponding to each sub-population. For example, in 3T3 cells, the integrated

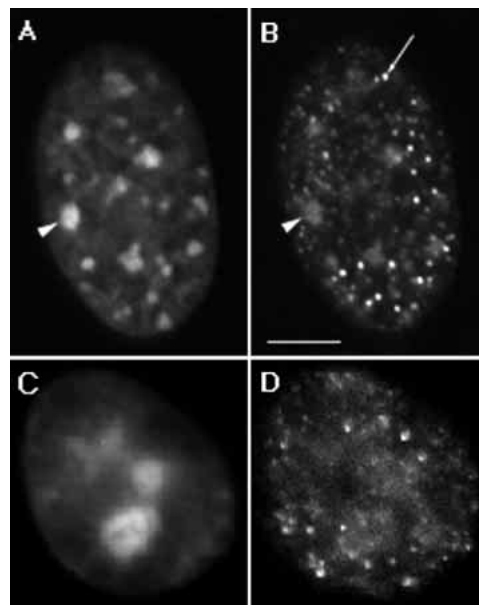


**Fig. 2.** A representative distribution of chromatin (A,C) and HMG-I protein (B,D) in the nucleus of a 3T3 cell (A,B) and of a HeLa cell (C,D). Cells were immunolabeled as above. In addition to a continuous diffuse labeling pattern, discrete small dots (arrow) and larger foci co-localized with condensed chromatin (arrowheads) can also be observed. Bar, 5  $\mu$ m.

intensities of the HMG-I dots, foci and continuous staining pattern account for 6-7, 9-19 and 70-86% of the total nuclear intensity and represent 1-3, 6-14 and 82-92% of the total number of stained pixels in the nucleus, respectively.

We also examined the distribution of HMG-I in two other human somatic cell lines. While the HMG-I immunolabeling pattern detected in transformed HEp-2 hepatocytes and 1BR fibroblasts was similar to that in HeLa and 3T3 cells, we noted variations in the number and intensity of the HMG-I dots. For instance, dots, which are very numerous in HEp-2 cells, are less abundant in 1BR cells and, in both cases, appear more intense than in HeLa or 3T3 cells (data not shown). Although the number of dots appears lower in 1BR cells than in 3T3 cells, they occupy a similar area (about 2% of the nuclear pixel number) indicating that their average size is increased. In addition, the integrated HMG-I intensity of the dots which, in 3T3 cells, represents 6% of the total nuclear fluorescence, increases to 15% in 1BR cells (standard error of the mean 0.5% and 6.8%, respectively,  $P=99\%$ ).

Confocal images ( $\Delta z=0.3 \mu$ m) of 3T3 and HeLa cells stained with propidium iodide (PI) and analyzed with the SPIMAC program showed a similar HMG-I distribution. A representative image of a 3T3 cell is shown in Fig. 4, together with the corresponding 2-D histogram. Analysis of the HMG-I signal with respect to PI fluorescence showed a similar subdivision into three sub-populations. As PI intercalates between the DNA base pairs without sequence specificity, its fluorescence intensity is directly proportional to the local DNA concentration. Therefore, the PI signal can be taken as reflecting the local density, or condensation state, of chromatin. As results obtained by conventional and confocal microscopy are qualitatively similar, subsequent studies were performed

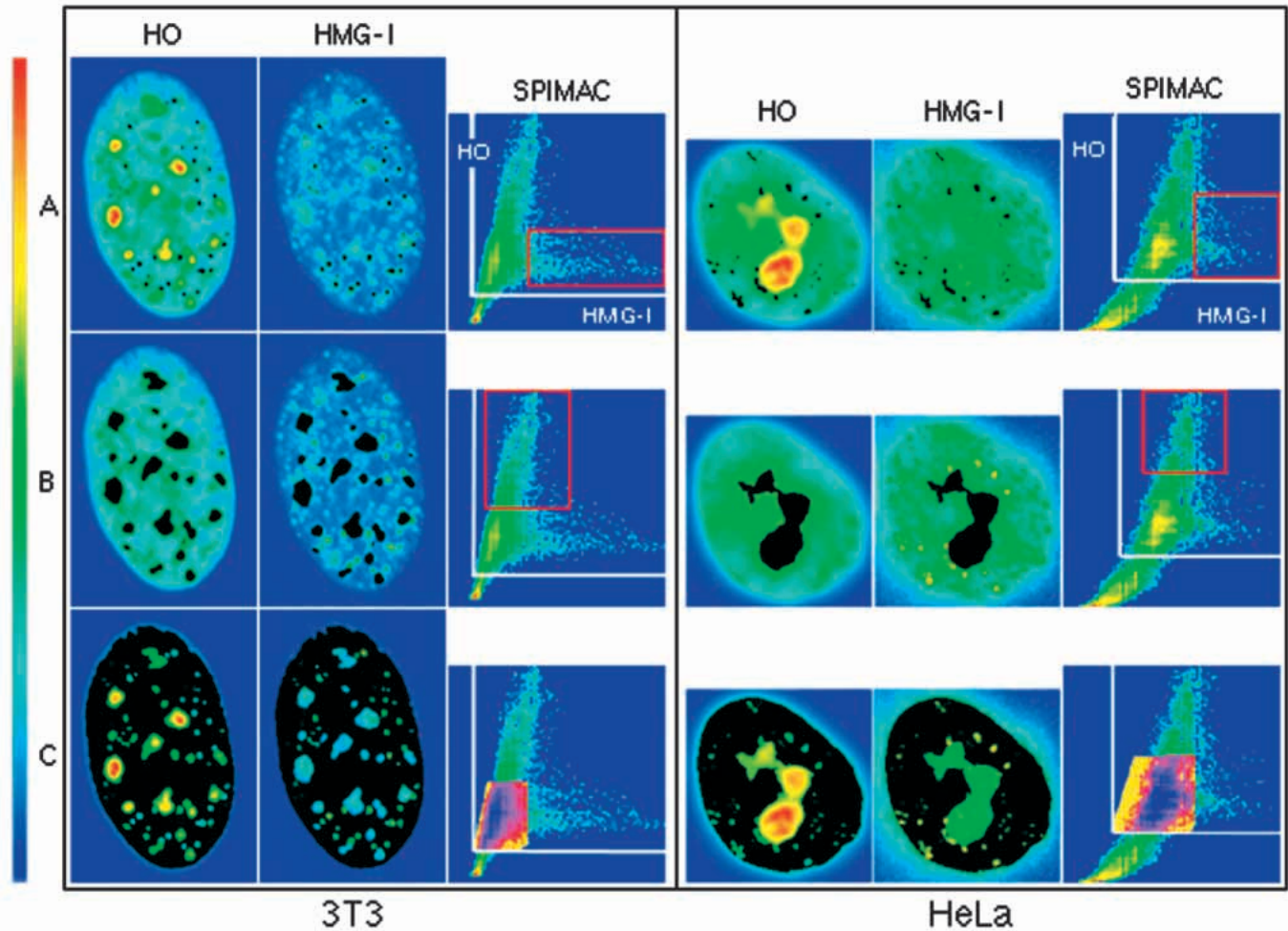


**Fig. 3.** Comparative SPIMAC analysis of the spatial distribution of HMG-I protein and chromatin in the nuclei of the 3T3 cell (left panel) and of the HeLa cell (right panel) shown in Fig. 2. In each panel, the columns representing Hoechst staining, HMG-I immunolabeling and the corresponding SPIMAC 2-D histograms are marked HO, HMG-I and SPIMAC, respectively. The  $x,y$  coordinates of each point in the 2-D histograms correspond to the normalized fluorescence intensity levels of the same pixel in the HMG-I and HO images, respectively. In each 2-D histogram, the two white lines separate low-intensity HO and HMG-I pixels located in the cytoplasm (bottom left) from higher-intensity pixels in the nucleus. The color scale on the left side (increasing from blue to red) is related to the pixel fluorescence intensity in the images, or the number of pixels of intensities  $x,y$  in the 2-D histograms. For each nucleus, three distinct nuclear sub-populations are delineated on the 2-D histograms by red rectangles (rows labeled A and B) or by a polygon (rows labeled C). The corresponding pixels appear in black on the HO and HMG-I images of the same row.

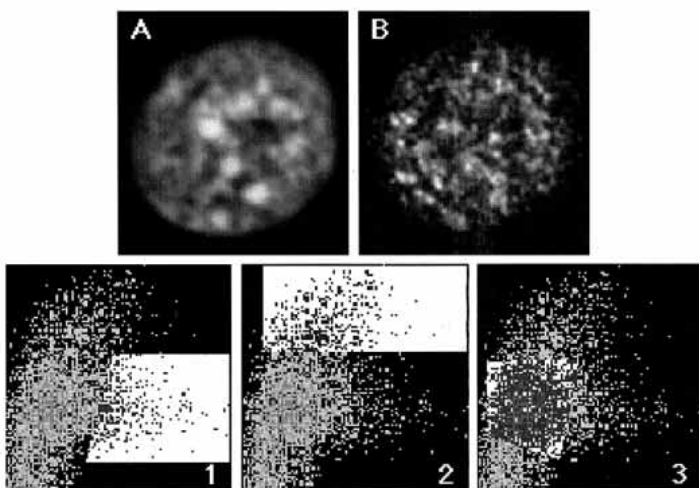


**Fig. 4.** Confocal section of a 3T3 cell nucleus stained with propidium iodide for chromatin (A) and with an FITC-conjugated secondary antibody for HMG-I (B). As in the case of images obtained by conventional microscopy, three HMG-I sub-populations can be evidenced from the SPIMAC 2-D histograms corresponding, respectively, to dots (1), foci (2) and to the continuous staining pattern (3).

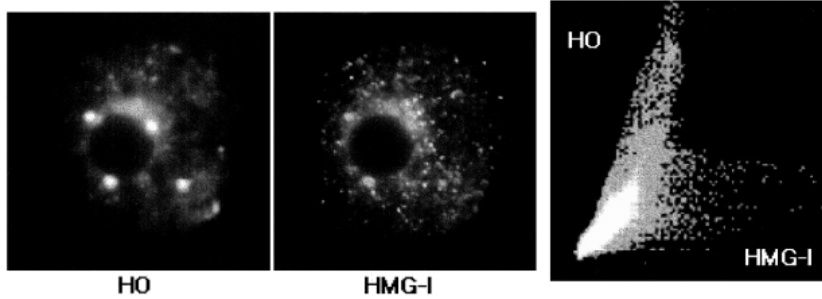


**Fig. 5.** A representative spatial distribution of chromatin and HMG-I in the germinal vesicle of a mouse oocyte. The corresponding SPIMAC 2-D histogram displays the same HMG-I distribution into three distinct sub-populations as in somatic cells.

using conventional microscopy, which is more sensitive than confocal microscopy.

We studied next the distribution of HMG-I in oocytes from 16-day-old mice. HMG-I was excluded from the nucleolus, which is already round and rather compact at that stage of growth (Borsuk et al., 1996). Significantly, three sub-populations similar to those observed in somatic cells can be distinguished in the extranucleolar space of the oocytes (Fig. 5).

In summary, indirect immunofluorescence labeling reveals the existence of three distinct HMG-I populations in nuclei. Although variations do exist, these sub-populations of HMG-I are consistently observed in all cell types studied and appear associated with different states of chromatin condensation. This discrete sub-nuclear localization pattern can be clearly evidenced by SPIMAC analysis, thus illustrating some of the advantages of this new program: the ability to discriminate on an objective basis between different sub-populations and to provide precise relationships between the intensities of two fluorescent labels. These possibilities have been used in the experiments described below.

### Nuclear HMG-I sites disappear progressively and selectively following treatment by DNase I and micrococcal nuclease

The three HMG-I sub-populations described above appear to be associated with regions of chromatin that differ in their level of condensation or in DNA density. Such a distribution might be accompanied by a selective sensitivity to nucleases. We tested this possibility by performing controlled digestions with DNase I or micrococcal nuclease. Fixed and permeabilized cells were incubated with DNase I (0.5 to 5  $\mu\text{g/ml}$ ) for 15 or 30 minutes and the total HO and HMG-I fluorescence intensity of individual nuclei (50 to 170 depending on the conditions) was measured as described in Materials and Methods.

Comparison of the mean values HO and HMG-I intensities with those of control undigested G1 cells are reported in Fig. 6 for 3T3 cells. The mean value of the HMG-I immunolabeling intensity decreased rapidly to 63 and 40% of the controls upon a 15-minute digestion by 0.5 and 1  $\mu\text{g/ml}$  DNase I, respectively. HO intensity remained essentially unchanged (Fig. 6A), indicating that the DNA was only mildly digested under these conditions. Increasing the incubation time from 15 to 30 minutes, as shown in Fig. 6B for 5  $\mu\text{g/ml}$  DNase I, led to a further decrease of the HMG-I and HO fluorescence signals, but which was again more rapid for HMG-I than for HO. The HMG-I signal also decreased faster than HO fluorescence in HeLa cells, although the overall effect was smaller than in 3T3 cells: after a 30-minute digestion with 5

$\mu\text{g/ml}$  DNase I, the mean DNA staining was only reduced to 77% and HMG-I labeling to 50% of their respective levels in untreated control cells (data not shown).

We then analyzed whether DNase I digestion affects the 3

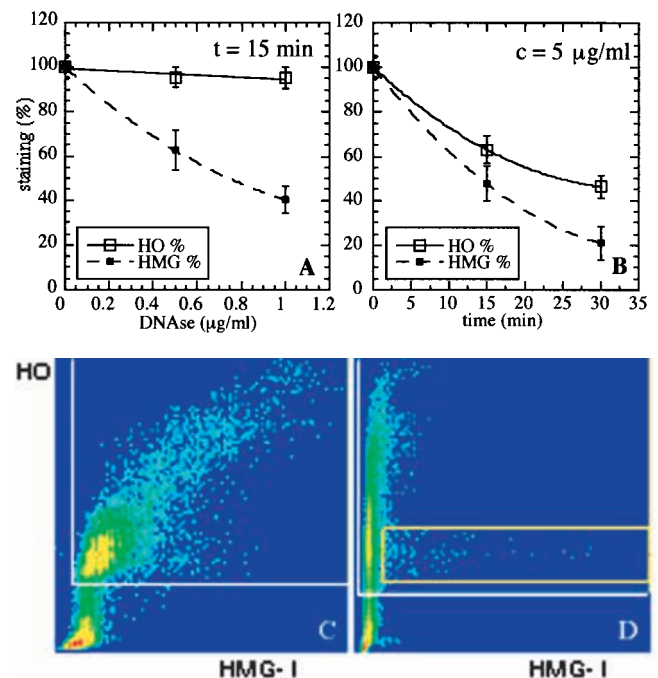


**Fig. 6.** Influence of DNase I treatment on HO and HMG-I fluorescence levels (A,B) and on the sub-nuclear distribution of HMG-I (C,D) in 3T3 nuclei. Fixed and permeabilized cells were incubated with 0.5 and 1.0  $\mu\text{g/ml}$  DNase I for 15 minutes (A), or for 15 and 30 minutes with 5  $\mu\text{g/ml}$  DNase I (B). Cells were then immunolabeled as above and nuclear HO and HMG-I fluorescence intensities were measured using a mask defined by thresholding the HO image as described in Materials and Methods. Each point represents the average of 50 to 170 cells. Results are expressed as a percentage of fluorescence intensity of control G1 cells without DNase I treatment. For DNase-treated samples, the HO intensity was averaged over all nuclei analyzed to compensate for the heterogeneity in digestion from cell to cell. Vertical bars correspond to the standard error of the mean ( $P=99\%$ ). A comparison of the SPIMAC 2-D histograms of a control cell (C) and of a cell treated with 5  $\mu\text{g/ml}$  DNase I for 15 minutes (D) shows the decreased staining of the HMG-I foci and of the continuous component and the persistence of the sub-population consisting of dots (yellow rectangle) after nuclease digestion. Note that the intensity values in C and D are derived from separate normalizations and cannot be compared.

HMG-I sub-populations equally. On images recorded with the  $\times 100$  objective, we observed a progressive and highly specific modification of the spatial distribution of HMG-I in nuclei as a function of DNase I digestion. Although we observed some variations in the effect of DNase I from cell to cell, a 15 to 30 minute incubation with 5  $\mu\text{g/ml}$  of DNase I resulted in the selective disappearance of two sub-populations, the diffuse continuous staining pattern and the foci co-localized with regions of condensed chromatin: only the high-intensity HMG-I dots remained visible in the nuclei of most cells. This is illustrated by the HMG-I/HO 2-D histogram of a 3T3 cell shown in Fig. 6D, where practically only bright dots concentrated on a horizontal line in the selected area of the histogram remain after digestion (compare with Fig. 6C). Except for these dots, the residual fluorescence intensity in the nucleus is only slightly higher than in the cytoplasm. A 30 minute digestion with 10  $\mu\text{g/ml}$  DNase I led to the complete disappearance of nuclear HMG-I labeling in all cells (data not shown).

We observed a similar progressive decrease of the nuclear

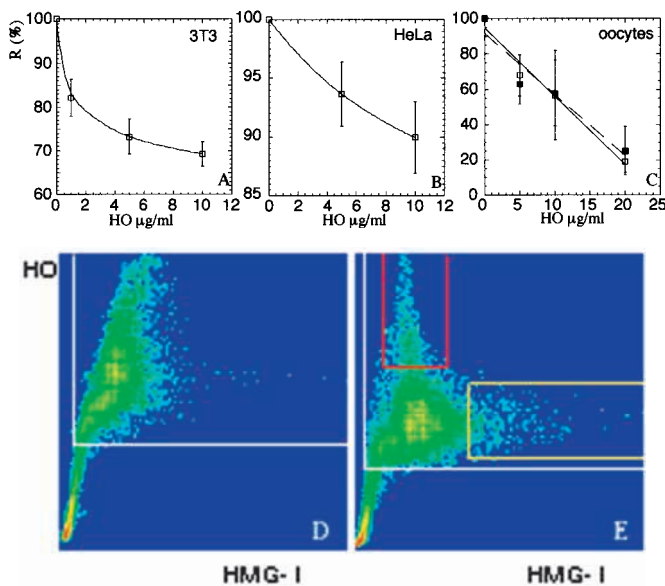


**Fig. 7.** Influence of the preincubation of living cells with Hoechst 33342 (HO) on HMG-I fluorescence levels (A,B,C) and on the sub-nuclear distribution of HMG-I (D,E). Living 3T3 cells (A), HeLa cells (B) or oocytes (C) were preincubated for 1 hour in the presence of HO in culture medium without serum, and then processed as above for immunolabeling. Quantification of the nuclear HMG-I fluorescence was performed using a mask defined on the HO image. The ordinate R represents the nuclear HMG-I fluorescence expressed as the percentage of the intensity in control cells without HO preincubation (note that scales are different in the three diagrams). 200 to 380 cells were analyzed for each experimental point. For oocytes, two different experiments were performed and 8 to 20 oocytes used for each experimental point. Vertical bars correspond to the standard error of the mean ( $P=99\%$ ). SPIMAC 2-D histograms are shown for a control HeLa cell (D) and for a HeLa cell treated with 5.0  $\mu\text{g/ml}$  HO for 1 hour (E). The intensity of the HMG-I signal corresponding to the foci decreases to a uniformly low value (red rectangle) while HMG-I dots persist after treatment (yellow rectangle). As in Fig. 5, absolute intensity values in the 2-D histograms in D and E cannot be compared.

HMG-I immunolabeling signal in 3T3 cells treated with increasing concentrations of micrococcal nuclease (MNase, 0.005 to 0.05 units/ml). Note that, in this case, the differential effect on the different HMG-I sub-populations was not as apparent as with DNase I: a mild MNase digestion led to a simultaneous decrease in the intensity of both dots and foci, but the dots persisted with a consistently higher contrast as compared to the foci when the MNase concentration was increased (data not shown).

### The HMG-I sub-populations are differentially displaced by preincubation of living cells with Hoechst 33342

One possible explanation for the selective modification of the nuclear distribution of HMG-I as a function of nuclease digestion is that the three sub-populations of HMG-I molecules are more or less tightly associated with DNA. If this were the case, they should be differentially affected by competition for DNA binding. As HMG-I has been shown to compete *in vitro* with drugs that specifically bind the minor groove of AT-rich sequences, such as Hoechst 33256 and distamycin A (Reeves and Nissen, 1990; Radic et al., 1992), we tested next whether Hoechst 33342 (HO, an analog of Hoechst 33256) could displace HMG-I molecules from their nuclear binding sites in living cells.

In the following experiments, living cells were preincubated

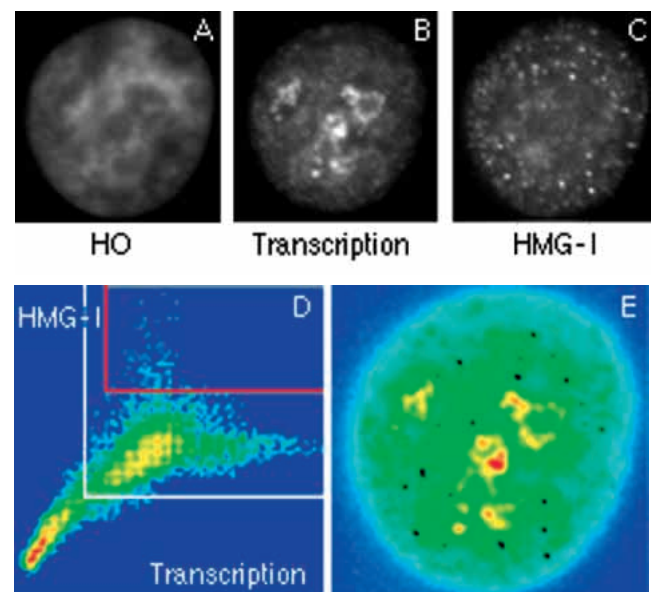


**Fig. 8.** Relative distribution of nascent RNAs and HMG-I protein in a HeLa cell nucleus. Cells grown on coverslips were microinjected with BrUTP, incubated 15 minutes and then processed as above for immunolabeling. (A) HO image. (B) Nascent RNAs were detected using a mouse monoclonal anti-BrdU antibody and a fluorescein-conjugated secondary antibody. (C) HMG-I was detected using a lissamine-rhodamine-conjugated secondary antibody. (D) A 2-D histogram of the relative distribution of transcription sites and HMG-I protein in the same cell. The white lines separate the pixels of the cytoplasm from those of the nucleus and the red lines isolate a sub-population corresponding to dots with high HMG-I fluorescence intensity. Pixels of HMG-I dots isolated on the 2-D histogram do not co-localize with sites of high accumulation of nascent RNAs (E).

with different concentrations of HO (1, 5 or 10  $\mu\text{g/ml}$ ), before being fixed and immunolabeled. Preliminary experiments showed that, at these concentrations, the nuclear HO intensity reached a plateau after 45 minutes of incubation and remained stable for at least 120 minutes. We therefore chose a 1 hour incubation time for these experiments.

When averaged over several optical fields, the mean total fluorescence intensity of HMG-I labeling (measured with a  $\times 20$  objective) decreased following incubation with increasing HO concentrations. Fig. 7 shows plots of R values (the ratio of the mean HMG-I fluorescence intensity in treated cells to that of controls without HO) as a function of HO concentration in different cell lines. In 3T3 cells, R reached 82% at 1  $\mu\text{g/ml}$  HO and decreased to 70% at 10  $\mu\text{g/ml}$  (Fig. 7A). The effect of HO was less important in HeLa cells as R only decreased to 90% after a 1 hour incubation in 10  $\mu\text{g/ml}$  HO (Fig. 7B). Higher concentrations of HO were found to be toxic to somatic cells and could not be tested. Again, similar results were observed in germinal cells: HMG-I was very efficiently displaced by HO in oocytes, with R decreasing to 60% and 20% at 10 and 20  $\mu\text{g/ml}$  HO, respectively (Fig. 7C).

As was the case for DNase I digestion, the different nuclear sub-populations of HMG-I accumulation sites were differently affected by preincubation with HO. The foci, corresponding to condensed chromatin, and, to a lower extent, the diffuse component were selectively displaced at the HO concentrations used (Fig. 7D and E). Note that these two sub-populations are also the most sensitive to nuclease digestion. In contrast, the intense HMG-I dots resistant to nuclease digestion appeared unaffected, as evidenced from the HMG-I/HO 2-D histogram of a HeLa cell shown in Fig. 7E. A similar preferential disappearance of the foci and of the diffuse signal was also observed in growing oocytes, where only HMG-I dots remained visible after incubation with HO (data not shown).

### **The most intense nuclear sites of HMG-I accumulation (dots) are not correlated with the most active transcription sites**

As previous results have shown that, by selectively binding to SARs, HMG-I might relieve *in vitro* histone H1-mediated transcriptional repression and that HMG-I is enriched in a sub-fraction of transcriptionally active chromatin (Zhao et al., 1993), we then asked whether HMG-I accumulation sites could be correlated *in situ* with sites of active transcription. Transcription sites were detected by visualizing BrU incorporated into nascent RNA chains after micro-injection of BrUTP, as shown in Fig. 8B in the case of a HeLa cell. In both HeLa and 3T3 cells, nascent RNAs generally appear in a more or less punctate pattern in the nucleoplasm and in nucleoli. Transcription foci are generally brighter in the nucleoli than in the nucleoplasm. All the nucleoli within an individual cell are not always systematically labeled. In the nucleoplasm, the punctate pattern is superimposed over a more uniform fluorescence signal.

In the 2-D histogram of a HeLa cell shown in Fig. 8D, the bright nucleolar RNA polymerase I-dependent transcription sites correspond to regions of low HMG-I intensity. In this case, there is no correlation between HMG-I immunofluorescence intensity and the level of BrU incorporation. A second region of this 2-D histogram,

delineated by the red rectangle, is formed by pixels of highest HMG-I intensity. This region extends over a medium range of transcription intensity. Visualization of the corresponding pixels on the transcription image (Fig. 8E) shows that they are scattered throughout the nucleoplasm. They correspond to the previously defined dots (compare C and E). The 2-D histogram (Fig. 8D) shows that there is no linear correlation in this sub-population between the intensities of the HMG-I and BrU immunofluorescence signals, i.e. the concentrations of HMG-I and incorporated BrU. The remaining part of the 2-D histogram represents pixels that correspond to HMG-I and BrU signals of medium intensities. This is by far the most abundant population which, on HMG-I images, corresponds to the previously defined foci and to the continuous fluorescence pattern. In this region, points are more or less clustered along a straight line, suggesting a broad linear correlation between HMG-I and BrU concentration.

Similar experiments performed in oocytes led to slightly different observations. As HMG-I labeling and transcription sites are essentially restricted to the extranucleolar space in these cells (Fig. 5 and unpublished results), the RNA/HMG-I 2-D histogram can be decomposed into two regions only. In the first region, the vast majority of the points are concentrated along a straight line, indicating a broad correlation between HMG-I and BrU intensities. The second region is composed of a smaller number of points characterized by a high HMG-I signal coupled to a moderate BrU signal, with no correlation between them (data not shown). As in the case of somatic cells, this last region corresponds to the intense dots localized in areas of low chromatin density.

## **DISCUSSION**

This work reports new results concerning the sub-nuclear distribution of HMG-I protein in human and murine cells, obtained with an original image analysis program developed in our laboratory, which allows a pixel-by-pixel analysis of the relationship between two independent fluorescence images of the same cell. Compared to an exclusively visual analysis, the SPIMAC software provides objective and semi-quantitative tools for the study of: (1) the distribution of a protein with respect to other nuclear components (in this study, chromatin or transcription sites); (2) its possible correlation with these components; (3) the definition of different sub-populations and their respective contribution to the overall signal; and (4) possible modifications of this pattern in response to various treatments (DNA digestion and competition with HO). Another advantage of this software is that it takes into account all the stained pixels, particularly those of low intensity. One must, however, bear in mind that any fluorescence-based analysis suffers from two main limitations: first, the resolution of optical microscopes (even when confocal) only allows the analysis of correlations on a scale that is considerably greater than molecular distances. Second, comparison of fluorescence intensities between various sub-domains is only indicative as factors other than the protein concentration, such as, for example, protein environment and accessibility to the antibody, may influence the fluorescence intensity.

We have used the SPIMAC program to perform a detailed analysis of the distribution of HMG-I in different cell types,

using an affinity-purified serum that recognizes the protein highly specifically. An unknown 120 kDa protein also detected in nuclear extracts from HeLa cells when low dilutions of the antibody are used most likely corresponds to another AT hook-containing protein, as a similar 120 kDa band is also detected by other sera raised against HMG-I as well as against a synthetic AT-hook peptide (unpublished results). This cross-reactivity does not affect our interpretation of the results as this protein is no longer detected upon serum dilution (Fig. 1A) and the specificity of the serum for HMG-I is further confirmed by results of the depletion experiment shown in Fig. 1G.

In all cells studied (somatic and germinal), HMG-I is exclusively located in the nucleus. We show here that this localization results from a complex distribution into intensively labeled dots and foci that are scattered over a diffuse network of lower fluorescence intensity extending throughout the whole nucleoplasm. The dots and foci most likely correspond to the punctate pattern previously observed by immunofluorescence in mouse Friend and human K562 erythroleukemia cells (Disney et al., 1989) and in mouse embryos and fetal fibroblasts (Thompson et al., 1995). In that respect, HMG-I distribution revealed by immunofluorescence resembles the complex (often punctate) distribution of several other nuclear proteins. For example non-DNA-bound factors involved in pre-mRNA processing, such as snRNPs (Carmo-Fonseca et al., 1991) and the splicing factors SC35 (Spector et al., 1991) or U2AF<sup>65</sup> (Gama-Carvalho et al., 1997), but also Pol II (Bregman et al., 1995; Zeng et al., 1997), are detected as discrete 'speckles' superimposed on a more diffuse component of lower intensity. Other transcription activators such as glucocorticoid receptors also accumulate in discrete nuclear foci (van Steensel et al., 1995).

The SPIMAC co-localization software provides additional quantitative information on this distribution: the most intensively labeled structures in 3T3 cells (small dots and larger foci) represent on average only about 1-3% and 6-14% of the total number of pixels and 6-7% and 9-19% of the total fluorescence intensity, respectively. In contrast, the diffusely distributed HMG-I sub-population occupies most (82-92%) of the pixels and, although of low mean intensity, accounts for 70-86% of the total fluorescence intensity. A similar situation is encountered in the case of the distribution of SC35: using another image analysis approach, Fay et al. (1997) showed that the intense 'speckles' contribute only a relatively minor part (20-30%) of the total SC35 immunofluorescence signal.

The comparison between HO (or PI) and HMG-I images shows that foci coincide perfectly with heterochromatic chromocenters, particularly numerous and well defined in mouse fibroblasts (Blau et al., 1983). Further analysis of these foci with the SPIMAC program indicates that HMG-I immunofluorescence labeling and HO (or PI) intensity are linearly correlated in these chromocenters. It is therefore tempting to speculate that the foci represent in situ binding of HMG-I on AT-rich satellite repeats clustered in regions of heterochromatin such as centromeres or telomeres. Indeed, HMG-I was first characterized on the basis of its specific binding to a 172 bp repeat of monkey  $\alpha$ -satellite DNA (Levinger and Varshavsky, 1982a,b; Strauss and Varshavsky, 1984) and was later localized to G/Q- and C-bands as well as

at telomeric and centromeric regions of human and mouse chromosomes (Disney et al., 1989).

On an HO/HMG-I 2-D histogram, the region corresponding to the diffuse HMG-I sub-population shows a less clear proportionality between HMG-I and HO intensities. We suggest that this population, which is associated with less condensed chromatin, represents HMG-I bound to randomly spaced AT-rich sequences in the genome, including dispersed satellite DNA sequences, SARs (Zhao et al., 1993) and possibly, the regulatory elements of certain genes (Thanos and Maniatis, 1992; John et al., 1995; Klein-Hessling et al., 1996; Ghersa et al., 1997).

In both somatic and germinal cells, the foci and, to a lower extent, the diffuse component share two specific properties: they are particularly sensitive to mild treatments with DNase I or MNase and they are preferentially displaced by pre-incubation of living cells with HO before fixation-permeabilization and immunolabeling. This strongly suggests that these two sub-populations correspond to DNA-bound HMG-I molecules since Hoechst 33342 (HO) specifically binds the minor groove of AT-rich DNA, as does its parent compound, Hoechst 33256, which was previously shown to compete with HMG-I for binding in vitro to mouse satellite DNA (Radic et al., 1992; Reeves and Nissen, 1990). The HMG-I foci localized in heterochromatin completely disappear under conditions where only about 30% of DNA is degraded. This unexpected result suggests that DNA regions bound by this HMG-I sub-population remain accessible to nucleases, and are therefore not deeply buried within condensed chromatin. Further studies will allow us to analyze in more detail the degree of folding and/or accessibility of the chromatin associated with this HMG-I population.

The third sub-population of HMG-I revealed in this study corresponds to small dispersed dots. Their high fluorescence intensity suggests that they correspond to a locally large accumulation of HMG-I molecules. It was therefore quite surprising to find that they do not correspond to high DNA concentrations, but are instead associated with areas of low local DNA density or of decondensed chromatin. In addition, this density is quite similar for all dots, suggesting that they reside in a rather uniform chromatin environment. This is particularly obvious in oocytes, where chromatin is heterogeneously dispersed within the wide nuclear volume.

Our finding that dots are displaced neither by mild nuclease digestion nor by HO leaves open the question of the nature of this sub-population: (i) dots could represent high molecular mass complexes of HMG-I molecules tightly bound to specific DNA sites and/or associated with particular chromatin conformations less accessible to nucleases and HO; (ii) alternatively this population might not be bound to DNA, corresponding instead to extrachromosomal accumulation sites. Their disappearance upon more advanced DNA digestion could be due to the overall disruption of nuclear architecture. As such, these hypothetical extrachromosomal HMG-I accumulation sites would be considerably more sensitive to nucleases than the SC35 speckles localized within interchromatin granules and perichromatin fibrils, which were previously shown to be resistant to extensive digestion by DNase I (100  $\mu$ g/ml for 2 hours at 25°C) (Spector et al., 1991). This observation would then favor the hypothesis that HMG-I dots are indeed DNA-bound.

To study further the possible functionalities associated with the different HMG-I sub-populations described in this study, we also analyzed their correlation with transcription sites revealed through BrU incorporation. In agreement with the results of other studies (Zheng et al., 1997; Fay et al., 1997), we found that Pol II-dependent transcription sites are distributed as a more or less continuous meshwork overlaid with more intense punctuations. In a double-labeling experiment, the transcription meshwork and the diffusely localized HMG-I sub-population were found to be co-localized. However, given the resolution of the optical microscope, the two signals will necessarily overlap and these results do not unambiguously establish a co-localization of transcription sites and HMG-I at the molecular level. A more definitive conclusion is that extranucleolar HMG-I dots do not correspond to sites of particularly active transcription and that, in these dots, HMG-I intensity is not correlated to BrU incorporation, i.e. to the rate of RNA synthesis. These observations apply to both interphase somatic cells and growing mouse oocytes arrested in prophase. The finding that dots are not associated with strong transcription sites suggests that they do not represent SAR-bound HMG-I molecules, as could be anticipated from previous studies showing that, at these sites, HMG-I-dependent displacement of histone H1 would lead to derepression of transcription (Zhao et al., 1993).

Alternatively, whether bound to DNA or not, the HMG-I dots could represent storage or recycling sites. Current views on the compartmentalization of eukaryotic nuclei suggest that the speckles revealed by immunofluorescence detection of certain nuclear proteins actually represent local and dynamic accumulations of these proteins, not necessarily attached to fixed structures, but fluctuating as a function of nuclear activity (Mistell et al., 1997; Zeng et al., 1997; Singer and Green, 1997). This also holds for DNA-binding proteins such as Pol II. In that respect, it is of interest to note that dots are more scarce and larger in 1BR cells, which have a slower growth rate and are presumably metabolically less active. This would parallel the decrease in number and increase in size of SC35 and Pol II speckles when transcriptional activity decreases (Bregman et al., 1995; Zeng et al., 1997; O'Keefe et al., 1994). Similarly, a reduction in the size of nuclear HMG-I punctuations was previously reported in fetal fibroblasts treated with trichostatin A, a histone deacetylase inhibitor which generally increases transcriptional activity (Thompson et al., 1995). This suggests that the distribution of HMG-I in the nucleus can be modulated as a function of the cellular proliferation and differentiation state. The availability of the imaging tools described in this report will allow us to address this possibility in future studies\*.

We thank Roger Fischer for his assistance in microinjection of cells, Pierre Adenot for his help in confocal microscopy and Danièle Chassoux for advices in cell culture. We are indebted to Christine Bouniol-Baly for fruitful discussions and careful reading of the manuscript.

\*In the process of revision of the present paper, a brief report by A. M. Martelli et al. was published in *J. Histochem. Cytochem.* (46, July 1998, 863-864) on the immunolocalization of HMG-I(Y) in HeLa and 3T3 cells. The results of the authors are basically consistent with ours.

## REFERENCES

- Blau, H. M., Chiu, C.-P. and Webster, C. (1983). Cytoplasmic activation of human nuclear genes in stable heterokaryons. *Cell* **32**, 1171-1180.
- Bouniol, C., Nguyen, E. and Debey, P. (1995). Endogenous transcription occurs at the 1-cell stage in the mouse embryo. *Exp. Cell Res.* **218**, 57-62.
- Borsuk, E., Vautier, D., Szöllösi, M. S., Besombes, D. and Debey, P. (1996). Development-dependent localization of nuclear antigens in growing mouse oocytes. *Mol. Reprod. Dev.* **43**, 376-386.
- Bregman, D. B., Du, L., van der Zee, S. and Warren, S. L. (1995). Transcription-dependent redistribution of the large subunit of RNA polymerase II to discrete nuclear domains. *J. Cell Biol.* **129**, 287-298.
- Bustin, M. and Reeves, R. (1996). High-Mobility-Group chromosomal proteins: architectural components that facilitate chromatin function. *Prog. Nucl. Acid Res. Mol. Biol.* **54**, 35-100.
- Carmo-Fonseca, M., Tollervey, D., Pepperkok, R., Barabino, S., Merdes, C., Brunner, C., Zamore, P. D., Green, M. R., Hurt, E. and Lamond, A. (1991). Mammalian nuclei contain foci which are highly enriched in components of the pre-mRNA splicing machinery. *EMBO J.* **10**, 195-206.
- Carmo-Fonseca, M., Pepperkok, R., Carvalho, M. T. and Lamond, A. (1992). Transcription-dependent colocalization of the U1, U2, U4/U6, and U5 snRNPs in coiled bodies. *J. Cell Biol.* **117**, 1-14.
- Debey, P., Szöllösi, M. S., Szöllösi, D., Vautier, D., Gironse, A. and Besombes, D. (1993). Competent mouse oocytes isolated from antral follicles exhibit different chromatin organization and follow different maturation dynamics. *Mol. Reprod. Dev.* **36**, 59-74.
- Demandoix, D. and Davoust, J. (1995). Multicolor analysis in confocal immunofluorescence microscopy. *J. Trace Microprobe Techn.* **13**, 217-225.
- Disney, J. E., Johnson, K. R., Magnuson, N. S., Sylvester, S. R. and Reeves, R. (1989). High-Mobility Group protein HMG-I localizes to G/Q- and C-bands of human and mouse chromosomes. *J. Cell Biol.* **109**, 1975-1982.
- Elton, T. S. and Reeves, R. (1986). Purification and postsynthetic modifications of Friend erythroleukemic cell high mobility group protein HMG-I. *Anal. Biochem.* **157**, 53-62.
- Falvo, J. V., Thanos, D. and Maniatis, T. (1995). Reversal of intrinsic DNA bends in the IFN- $\beta$  gene enhancer by transcription factors and the architectural protein HMG I(Y). *Cell* **83**, 1101-1111.
- Fay, F. S., Taneja, K. L., Shenoy, S., Lifshitz, L. and Singer, R. H. (1997). Quantitative Digital analysis of diffuse and concentrated nuclear distributions of nascent transcripts, SC35 and poly(A). *Exp. cell Res.* **231**, 27-37.
- French, S. A., Schmidt, M. C. and Glorioso, J. C. (1996). Involvement of a High-Mobility-Group Protein in the transcriptional activity of herpes simplex virus latency-active promoter 2. *Mol. Cell. Biol.* **16**, 5393-5399.
- Gama-Carvalho, M., Krauss, R. D., Chiang, L., Valcarcel, J., Green, M. R. and Carmo-Fonseca, M. (1997). Targeting of U2AF<sup>65</sup> to sites of active splicing in the nucleus. *J. Cell Biol.* **137**, 975-987.
- Ghersa, P., Whelan, J., Cambet, Y., DeLamararter, J. F. and van Huijsduijnen, R. H. (1997). Distamycin prolongs E-selectin expression by interacting with a specific NF- $\kappa$ B-HMG-I(Y) binding site in the promoter. *Nucl. Acids Res.* **25**, 339-346.
- Izaurralde, E., Käs, E. and Laemmli, U. K. (1989). Highly preferential nucleation of histone H1 assembly on scaffold-associated regions. *J. Mol. Biol.* **210**, 573-585.
- John, S., Reeves, R. B., Lin, J.-X., Child, R., Leiden, J. M., Thompson, C. B. and Leonard, W. J. (1995). Regulation of cell-type-specific interleukin-2 receptor  $\alpha$ -chain gene expression: potential role of physical interactions between Elf-1, HMG-I(Y), and NF- $\kappa$ B family proteins. *Mol. Cell. Biol.* **15**, 1786-1796.
- Käs, E., Izaurralde, E. and Laemmli, U. K. (1989). Specific inhibition of DNA binding to nuclear scaffolds and histone H1 by distamycin. *J. Mol. Biol.* **210**, 587-599.
- Käs, E., Poljak, L., Adachi, Y. and Laemmli, U. K. (1993). A model for chromatin opening: stimulation of topoisomerase II and restriction enzyme cleavage of chromatin by distamycin. *EMBO J.* **12**, 115-126.
- Klein-Hessling, S., Schneider, G., Heinfing, A., Chuvpilo, S. and Serfling, E. (1996). HMG I(Y) interferes with the DNA binding of NF-AT factors and the induction of the interleukin 4 promoter in T cells. *Proc. Nat. Acad. Sci. USA* **93**, 15311-15316.
- Leger, H., Sock, E., Renner, K., Grummt, F. and Wegner, M. (1995). Functional interaction between the POU domain protein Tst-1/Oct-6 and the high-mobility-group protein HMG-I/Y. *Mol. Cell. Biol.* **15**, 3738-3747.
- Levinger, L. and Varshavsky, A. (1982a). Selective arrangement of

- ubiquitinated and D1 protein-containing nucleosomes with the *Drosophila* genome. *Cell* **28**, 375-385.
- Levinger, L. and Varshavsky, A.** (1982b). Protein D1 preferentially binds (A+T)-rich DNA in vitro and is a component of *Drosophila melanogaster* nucleosomes containing (A+T)-rich satellite DNA. *Proc. Nat. Acad. Sci. USA* **79**, 7152-7156.
- Maher, J. F. and Nathans, D.** (1996). Multivalent DNA-binding properties of the HMG-I proteins. *Proc. Nat. Acad. Sci. USA* **93**, 6716-6720.
- Mistell, T., Caceres, J. F. and Spector, D. L.** (1997). The dynamics of a pre-mRNA splicing factor in living cells. *Nature* **387**, 523-527.
- O'Keefe, R. T., Mayeda, A., Sadowski, C. L., Krainer, A. R. and Spector, D.** (1994). Disruption of Pre-mRNA splicing in vivo results in reorganization of splicing factors. *J. Cell Biol.* **124**, 249-260.
- Radic, M. Z., Saghbini, M., Elton, T. S., Reeves, R. and Hamkalo, B. A.** (1992). Hoechst 33258, distamycin A, and high mobility group protein I (HMG-I) compete for binding to mouse satellite DNA. *Chromosoma* **101**, 602-608.
- Reeves, R. and Nissen, M. S.** (1990). The A. T-DNA-binding domain of mammalian high mobility group I chromosomal proteins. *J. Biol. Chem.* **265**, 8573-8582.
- Saitoh, Y. and Laemmli, U. K.** (1994). Metaphase chromosome structure: bands arise from a differential folding path of the highly AT-Rich scaffold. *Cell* **76**, 609-622.
- Singer, R. H. and Green, M. R.** (1997). Compartmentalization of eukaryotic gene expression: causes and effect. *Cell* **91**, 29294.
- Spector, D. L., Fu, X.-D. and Maniatis, T.** (1991). Association between distinct pre-mRNA splicing components and the cell nucleus. *EMBO J.* **10**, 3467-3481.
- Strauss, F. and Varshavsky, A.** (1984). A protein binds to a satellite DNA repeat at three specific sites that would be brought into mutual proximity by DNA folding in the nucleosome. *Cell* **37**, 889-901.
- Taneja, K. L., Lifshitz, M., Fay, F. S. and Singer, R. H.** (1992). Poly(A) RNA codistribution with microfilaments: evaluation by in situ hybridization and quantitative digital imaging microscopy. *J. Cell Biol.* **119**, 1245-1260.
- Thanos, D. and Maniatis, T.** (1992). The high mobility group protein HMG-I(Y) is required for NF-kB-dependent virus induction of the human IFN- $\beta$  gene. *Cell* **71**, 777-789.
- Thanos, D. and Maniatis, T.** (1995). Virus induction of human IFN- $\beta$  gene expression requires the assembly on an enhancosome. *Cell* **83**, 1091-1110.
- Thompson, E. M., Legouy, E., Christians, E. and Renard, J. P.** (1995). Progressive maturation of chromatin structure regulates HSP70. 1 gene expression in the preimplantation mouse embryo. *Development* **121**, 3425-3437.
- van Steensel, B., Brink, M., van der Meulen, K., van Binnendijk, E. P., Wansink, D. G., de Jong, L., de Kloet, E. R. and van Driel, R.** (1995). Localization of the glucocorticoid receptors in discrete clusters in the cell nucleus. *J. Cell Sci.* **108**, 3003-3011.
- Wansink, D. G., Schul, W., van der Kraan, I., van Steensel, B., van Driel, R. and de Jong, L.** (1993). Fluorescent labeling of nascent RNA reveals transcription by RNA polymerase II in domains scattered throughout the nucleus. *J. Cell Biol.* **122**, 283-293.
- Wegner, M. and Grummt, F.** (1990). Netropsin, Distamycin and Berenil interact differentially with a high-affinity binding site for the high mobility group protein HMG-I. *Biochim. Biophys. Res. Commun.* **166**, 1110-1117.
- Yie, J., Liang, S., Merika, M. and Thanos, D.** (1997). Intra- and intermolecular cooperative binding of high-mobility-group protein I(Y) to the beta-interferon promoter. *Mol. Cell. Biol.* **17**, 3649-3662.
- Zhao, K., Käs, E., Gonzalez, E. and Laemmli, U. K.** (1993). SAR-dependent mobilization of histone H1 by HMG-I/Y *in vitro*: HMG-I/Y is enriched in H1-depleted chromatin. *EMBO J.* **12**, 3237-3247.
- Zeng, C., Kim, E., Warren, S. L. and Berget, S. M.** (1997). Dynamic relocation of transcription and splicing factors dependent upon transcriptional activity. *EMBO J.* **16**, 1401-1412.